Structural characterization of nanoparticulate GaN-ZnO electrode for artificial photosynthesis

The artificial photosynthesis technology known as the Honda-Fujishima effect, which produces oxygen and hydrogen or organic energy from sunlight, is an effective energy and environmental technology. The key component for the increasing the efficiency of this reaction system is the anode electrode, generally composed of a photocatalyst on a glass substrate coated by electrically conductive fluorine-doped tin oxide (FTO).

Recently, we applied aerosol-type nanoparticle deposition (NPD) techniques to form a GaN-ZnO electrode, and by controlling the deposition conditions, we obtained films with a narrower band gap than the raw material powder. We confirmed that the films produced a current approximately 100 times larger than those produced by conventional processes. In this study, we analyzed the structural difference between such a high-current film and the raw powder by applying XRD, HAXPES, and XAFS techniques using SPring-8 **BL16XU** and **BL16B2** (Sunbeam) beamlines. These results are discussed with those of a first-principles simulation [1].

The nanoparticle deposition equipment [2,3] was composed of an aerosol-generation system, a deposition chamber, and a vacuum system. Raw ceramic powder was set in the aerosol-generation system. Then, a pressurized carrier gas was introduced into the vessel to transfer the generated aerosol from the nozzle to the substrate in the deposition chamber. This method is suitable for forming a nanoparticle crystal film of complex ceramic.

A GaN-ZnO-based material is a solid solution of hexagonal wurtzite structure crystals that continuously changes its composition as Ga-Zn and N-O are substituted in the crystal structure. It is known that a GaN-ZnO solid solution has a narrower band gap than pure GaN or ZnO, and its absorption wavelength edge expands to the long-wavelength side as the amount of ZnO dissolved into the GaN increases [4].

To synthesize a $Ga_{1-x}Zn_xN_{1-x}O_x$ ($x = 0$ to 1) solid solution, we adopted a general solid-state reaction using oxide raw materials (Ga_2O_3, ZnO) at a high temperature (1123 K) in an ammonia gas flow. It was, however, difficult to increase the amount of ZnO to more than $x = 0.45$.

In the NPD deposition, we applied two types of condition. As the first condition, nitrogen carrier gas with a speed of 50 m/s was used to transfer the source powder to the substrate, and the resulting film is called NPD_0. As the second condition, helium gas with a speed of 100 m/s was used and the film is called NPD*.

Figure 1 shows the appearances of the raw material powder with $x = 0.45$, and the NPD_0 film and NPD* film formed on an FTO substrate using this raw material powder. In the same figure, the Kubelka-Munk values are plotted, which were obtained from the diffuse reflectance spectrum by using UV and visible light. The reflection absorption edge of the raw material powder was at 490 nm (band gap: 2.53 eV) and that of the NPD_0 film was at 545 nm (band gap: 2.27 eV). The raw material powder and the NPD_0 film have almost the same yellow color, and a small difference in the band gap values was detected. The NPD* film is brown and its absorption edge was at 635 nm (band gap: 1.97 eV), which is significantly smaller than that for the original raw powder.

Figure 2(a) shows the hard X-ray photoelectron spectroscopy (HAXPES) spectra near the top of the valence band for the NPD* films with $x = 0$, 0.24, 0.45, and 1. The end of each spectrum is a valence band maximum (VBM). According to the figure, the VBM increased with increasing ZnO content, which indicates that the electron level of the solid solution is highest at $x = 0.45$. Also, we observed similar dependences for the raw material powder and the NPD_0 film.

We performed XAFS measurement at the Ga *K*-edge and Zn *K*-edge of the raw powder and NPD* film with the composition $x = 0.45$. The XAFS spectrum $\chi(k)$ was extracted from the measured data. In Fig. 2, the Fourier transformed Ga $\chi(R)$ with the compositions $x = 0$ (b) and 0.45 (c) are shown. The peaks in the figures correspond to the bond

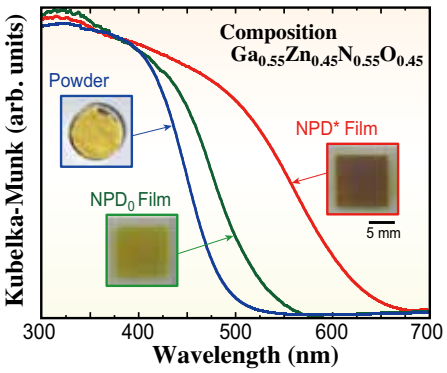

Fig. 1. Kubelka-Munk values of the raw material powder (blue), NPD_0 film (green), and NPD* film (red) for the composition $x = 0.45$ obtained from the diffuse reflectance spectra measured by using UV and visible light.

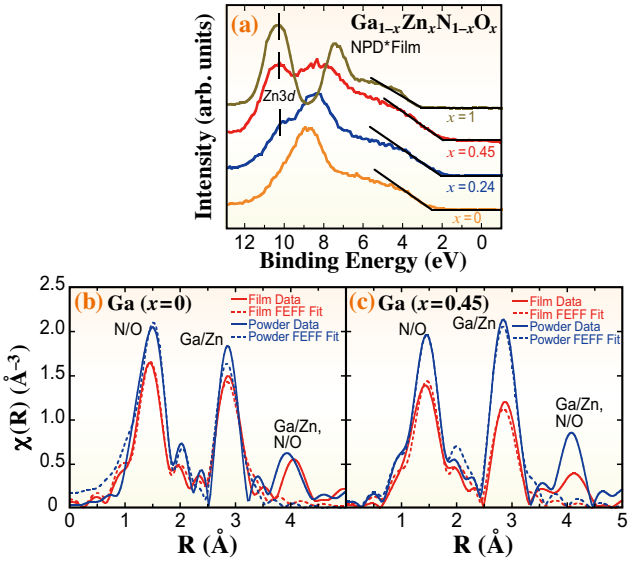

Fig. 2. **(a)** Hard X-ray photoelectron spectroscopy (HAXPES) spectra around the top of the valence band for the NPD* film. Effective bond length distributions of the raw material powder and the NPD* film for compositions $x = 0$ **(b)** and 0.45 **(c)** obtained from Ga *K*-edge XAFS.

length and the intensity decreases with the structural disorder. For the composition of $x = 0$ (b), the intensity of the first nearest peak, which corresponds to the Ga-(N/O) bond, was lower for the NPD* film than for the powder. For the composition of $x = 0.45$ (c), in addition to the first nearest peak, the intensity was also lower for the second nearest peak, which corresponds to the Ga-(Ga/Zn) bond. From these results, we confirmed that in the NPD* film, the atomic disorder is greater than that in the raw material powder, and the disorder is further increased by the substitution of ZnO. The most likely reason for the increase in the atomic disorder is the local strain due to the different ion radii of Ga and Zn, which is largest for the composition $x = 0.45$, and the soft distortion occurring in the film formation process.

As the increase in atomic disorder may have contributed to the decrease in the band gap, we carried out a first-principles simulation using the crystal structure model with composition $x = 0.5$. To reproduce the crystal disorder, we used the model of the partial crystal structure shown in Fig. 3(a). In the model, we introduced the displacement *d* in the *c*-axis direction for the bonding pair composed of a given cation and a neighboring anion. From the simulation, we found that the band gap energy decreases as the displacement increases, regardless of the displacement direction. In this simulation, when a pair of atoms was displaced by only 0.2 Å, the band gap energy decreased by approximately 0.2 to 0.3 eV. Figure 3(b) shows schematic diagrams of the electronic structure with and without the displacement. With the displacement, the conduction band formed by 4*s* and 4*p* orbitals of Ga and Zn expands and the conduction band minimum (CBM) is lowered, which results in the decrease in the band gap.

As described above, we have proven that the application of the NPD process to photocatalyst materials can form nanoparticulate films with a narrower band gap, and this method is applicable to various other photocatalysts.

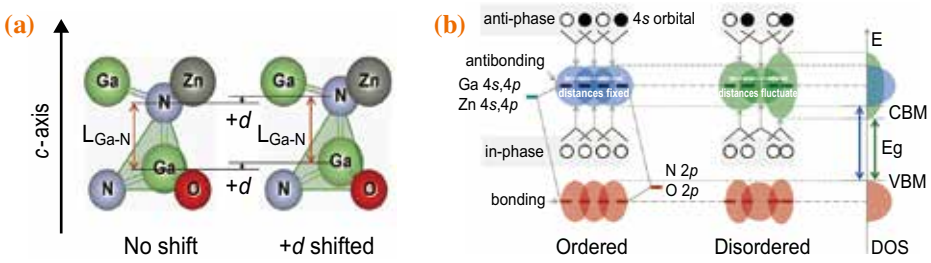

Fig. 3. **(a)** Partial structure with the atom displacement in the crystal model. **(b)** Schematic diagrams explaining the decrease in the band gap energy due to the displacement of the atom positions.

Yoshihiko Imanaka* and Naoki Awaji

Fujitsu Laboratories, Ltd.

*Email: Imanaka@jp.fujitsu.com

References

[1] *Y. Imanaka, T. Anazawa, T. Manabe, H. Amada, S. Ido, F. Kumasaka, N. Awaji, Ga. Sánchez-Santolino, R. Ishikawa and Y. Ikuhara: Sci. Rep.* ***6*** *(2016) 35593.*
[2] Y. Imanaka *et al.*: Ad. Eng. Mat. **15** (2013) 1129.
[3] Y. Imanaka *et al.*: J. Nanopart. Res. **18** (2016) 102.
[4] K. Maeda and K. Domen: J. Phys. Chem. C **111** (2007) 7851.